Energy and Buildings 77 (2014) 256–269

Contents lists available at ScienceDirect

Energy and Buildings

journal homepage: www.elsevier.com/locate/enbuild

Estimation of an incipient fault using an adaptive neurofuzzy sliding-mode observer☆

Yimin Zhou[a,b,*], Jingjing Liu[a,c], Arthur L. Dexter[a]

[a] Department of Engineering Science, University of Oxford, Oxford, UK
[b] Shenzhen Institutes of Advanced Technology, Chinese Academy of Sciences, China
[c] Kuang-Chi Institute of Advanced Technology, Shenzhen, China

ARTICLE INFO

Article history:
Received 2 January 2014
Accepted 1 February 2014
Available online 8 April 2014

Keywords:
Fuzzy relational sliding mode observer
On-line learning scheme
Cooling-coil
Actuator fault
Flow reduction fault

ABSTRACT

A fault, especially an incipient fault has to be detected as early as possible to avoid serious damage occurring in the controlled system. A fuzzy relational sliding mode observer (FRSMO) is proposed to estimate the magnitude of slowly evolving faults in information-poor and non-linear systems. To reduce modelling errors, an on-line learning fault identification scheme is used to update the model and identify the fault in a periodical mode. The performance of the proposed methods is evaluated using a cooling-coil subsystem of an air-conditioning plant in a simulated environment. The simulation results of the actuator fault and flow reduction fault estimation confirm the effectiveness of the proposed methods.

1. Introduction

1.1. Brief introduction

There has been considerable interest in fault detection and identification in recent years due to the increasing complexity and degree of automation of technical processes. A more suitable strategy of using knowledge-based techniques instead of traditional linearization techniques is used to produce a model of a non-linear system. The neurofuzzy approach is a good alternative way of describing the relationship between the input and output variables.

Along with the complexity of modern control systems, the issue of availability, cost efficiency, reliability, operating safety and environmental protection are of major importance. The consequence of faults can be extremely serious for safety-critical systems. A fault is defined as an unacceptable deviation from the nominal system behaviour [1]. It can disturb the normal operation of a system, thus causing an unacceptable deterioration of the performance of the system or even leading to dangerous consequences. Early indications of faults can help avoid drastic conditions such as system breakdown, mission abortion and catastrophes [2]. Moreover, the size of the fault needs to be known so as to reduce more energy consumption [3] and improve efficiencies, as seen in chemical composition procedure processes, air conditioning systems and biological industries.

Fault diagnosis has been recognized as an independent discipline in the last decades and many methods have been developed. In early times, hardware redundancy was regarded as the main method to diagnose faults. Along with the development of science and technology in control engineering, hardware redundancy has gradually been replaced by analytical redundancy due to the requirement of extra equipment and maintenance costs.

Fault diagnosis using analytical redundancy is currently a subject of extensive research and numerous surveys can be found in the literature [4–10]. In analytical redundancy schemes, signals (**residuals**) which carry the fault information are used for diagnosis. The residual should be zero when the system is normal, and should diverge from zero when a fault occurs in the system. This zero and non-zero property of the residual is used to determine the existence of the fault in the monitored system. The residual signals are normally generated by comparing the measured signals with their estimates obtained from a model of the fault-free system. There are three commonly used methods for residual generation in practice [11]:

(1) Comparison between the measured system outputs and prediction from a nominal model of the system.
(2) Comparison between the parameters of the nominal plant model and those of a model of the plant estimated on-line.
(3) Examination of the measured signals, which carry the fault information.

☆ The work was completed when Dr. Zhou was a graduate student in the Department of Engineering Science at the University of Oxford.

* Corresponding author at: Shenzhen Institutes of Advanced Technology, Chinese Academy of Sciences, China. Tel.: +86 755 86392152.
E-mail addresses: ym.zhou@siat.ac.cn (Y. Zhou), jingjing.liu@eng.ox.ac.uk (J. Liu).

0378-7788/$ – see front matter © 2014 Elsevier B.V. All rights reserved.
http://dx.doi.org/10.1016/j.enbuild.2014.02.001

1.2. Residual generation

(1) The residual is the difference between the measured output from the plant and the model: $r_1 = y - \hat{y}$

The nominal system behaviour is described by a fault-free model. Once a fault occurs in the system, the output of the model $\hat{y}$ is different from the output y of the plant. The residual $(r_i = y_i - \hat{y}_i)$ in the monitored system includes fault information, which can be used for fault diagnosis:

$$r_i = 0, \quad \text{if} \quad f_i = 0; \quad r_i \neq 0, \quad \text{if} \quad f_i \neq 0 \tag{1}$$

A diagram of this method of residual generation is shown in Fig. 1, where $(f_1, \ldots, f_m)$ represent the different sizes of the same fault f_i. Multiple models have to be developed to obtain the degree of the faults.

A robust adaptive unknown input observer has been proposed [12] to diagnose time-varying actuator faults in a second-order dynamic system. The residual can be used to generate an on-line estimate of the fault $\hat{f}(t)$ if it is an actuator fault. An adaptive threshold is added to reduce the computational burden associated with fault isolation. However, this scheme is only developed for an incipient or abrupt actuator fault in a linear dynamic system and it cannot be used to identify the size of a component fault, which involves fault isolation.

Fault isolation and estimation in linear continuous-time and discrete-time systems has also been considered in [13]. An estimator of the faults which has a linear relationship to the output is developed based on the measured outputs in the system. In this scheme, the estimation of the faults is dependent largely on the relationship between the faults and the outputs. It cannot be applied to general systems in which the fault is not directly related to the output of the model.

(2) The residual is the difference between a nominal parameter vector and a fault parameter vector: $r_2 = \theta - \hat{\theta}$

Robust parameter estimation approaches are discussed in survey paper by Frank and his co-workers [2,5]. If there is a fault in the system, the model of the nominal system is updated based on the faulty input/output measurements. The differences between the nominal parameter vector and that obtained from the faulty system can be regarded as the fault symptoms. A diagram of the residual generation is illustrated in Fig. 2. For instance, if there is fouling inside the pipes in a heating subsystem, the value of the heat transfer coefficient can be used to estimate the thickness of the fouling.

Dexter and Ngo described a method [14] of diagnosing incipient faults with multiple reference models for different fault sizes. The scheme is divided into two phases: fault elimination and fault classification. In the first phase, the fault symptom signals are compared to different faulty models to eliminate any ambiguous evidence. In the second phase, the diagnostic scheme identifies the types of faults. The level of the fault can be detected by comparing the parameter values of the nominal model and those of the faulty models. If the diagnosis fails to generate unambiguous belief in a single fault, the diagnosis will be repeated. This scheme generates more precise results of the fault estimation by reducing the number of the models. In addition, it greatly reduces the chance of false alarms by taking account of the uncertainties. However, the exact magnitude of the fault cannot be obtained and only roughly grade of the fault is obtained from this scheme.

(3) The output residual r_3 drives an observer which estimates the size of the fault

In this case, the fault is estimated directly based on an observer. The diagram of the residual generation is depicted in Fig. 3.

Frank and Ding published a paper on observer-based fault detection systems [6]. Sliding mode observers (SMO) [15] have been applied to linear systems for fault estimation [16]. The model of the plant is transformed into a form such that the output can be described as part of the state vector of the model. A residual is generated from the state error between the estimated state from the model and the actual state of the system. The fault estimation is directly obtained from the error system if the error approximates to zero gradually [17]. The sliding mode observer scheme has the advantage that it can deal with the unmodelled disturbances and uncertainties in the system. There are two main design methods for obtaining the fault estimate: one is based on the hyperstability concept whilst the second uses Lyapunov methods [18]. However, the extension of the method of fault estimation in general nonlinear systems has not been discussed.

Faults can be classified into several categories. From the system structure point of view, faults can be divided into component faults, sensor faults and actuator faults. From the time dependence of faults, they can be classified into incipient faults (also called soft faults, the parameters of the components are changing due to the variation in the ambient temperature and environment, etc.), abrupt faults (large bias occurs in the monitored signal) and intermittent faults (ageing or not enough capacity or poor connection) [19].

Once an abrupt fault occurs in the system, it is easy to be determined and located. Appropriate measures can be taken to eliminate the fault without any further investigation. Degradation or incipient faults, however, are difficult to be detected at an early stage because they change slowly. It is necessary to identify the magnitude of the incipient fault in case a significant loss of performance occurs without being noticed.

A survey of the approaches using parity space in fault diagnosis can be found in [20]. Parity space techniques provide less flexibility when compared with parameter estimation approaches [21,22]. Model-based fault diagnosis schemes are considered and summarized in the following papers: parameter estimation [23], fault-detection filters [24,25], observer-based approaches [26–29] and neural networks [30–32]. A sliding mode observer-based fault detection and estimation with nonlinear networked control system is proposed in [33–35].

A practical solution of detecting a fault in a nonlinear system where four thrusters are used to generate torques in a benchmark satellite system Mars Express (Mex), subject to model uncertainties and sensor noise is proposed in [36]. A sliding mode observer is designed to generate residual signals by filtering the equivalent signal. A threshold is designed to identify the fault from the residual signal. A faulty thruster can be isolated by the method of directional cosine evaluation. The error between the measured angular velocity and the estimated angular velocity is used to be the sliding mode surface. However, it only focuses on the fault detection without obtaining the magnitude of the fault.

T-S fuzzy identification and control was proposed in [37] and T-S fuzzy reference models are used in simultaneous, multiplicative actuator and sensor fault diagnosis and estimation with linear state observers [38]. An on-line fault tolerant control strategy is proposed in [39]. By correcting the faulty measurements with a final correcting factor, the fault detection and correction can be achieved. A development of easy-to-use tool for fault detection and diagnosis in air-conditioning system is described in [40]. Nonlinear system parameter fault estimation via sliding mode observer and neural network fault approximation is discussed in [41]. However, neural estimator and sliding mode observer is designed to deal with a single input and single output system. The fault is directly estimated by RBF neural networks in a model-free system.

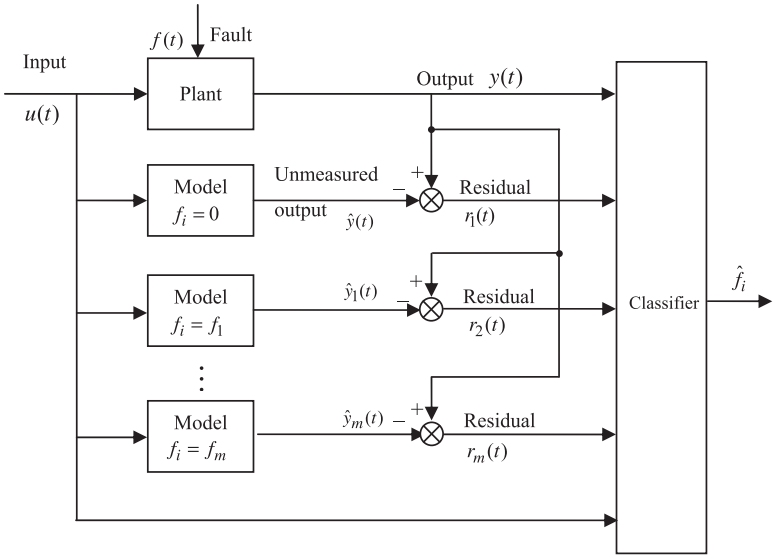

Fig. 1. Residual generation from the output.

It can be only applied in a special from of nonlinear SISO systems.

In Chapter 11 [16], it summarizes the sliding mode observer design for fault detection and isolation leading to fault tolerant control. The fault can be reconstructed for obtaining the size perfectly, which can be dealt with actuator faults and sensor faults. Details of the fault estimation with sliding mode design are presented. Castillo et al. propose a robust fault observer to detect and isolate the fault with sliding mode observer [42]. A nonlinear discrete observer is used to predict the output measurement with linearized output functions. After the fault occurrence, it is estimated by a statistical model created using PCA. Sliding modes are designed in a nonlinear observer to cope with the parameter uncertainties in the system. The design process is very complicated since model-based approach for state estimation in robust observer with the contribution from sliding mode and data-driven approach for fault isolation have to be designed.

Wu and Saif propose a neural-fuzzy sliding mode observer for fault diagnosis in [43], the system is a combination of linearized subsystems. It can only deal with the detection with the occurrence of the fault in the system. Faults are regarded as unknown inputs in [44], and multiple sliding mode observers are designed to estimate the unknown inputs through nonlinear transformation. The estimated unknown inputs share the same reconstruction structure

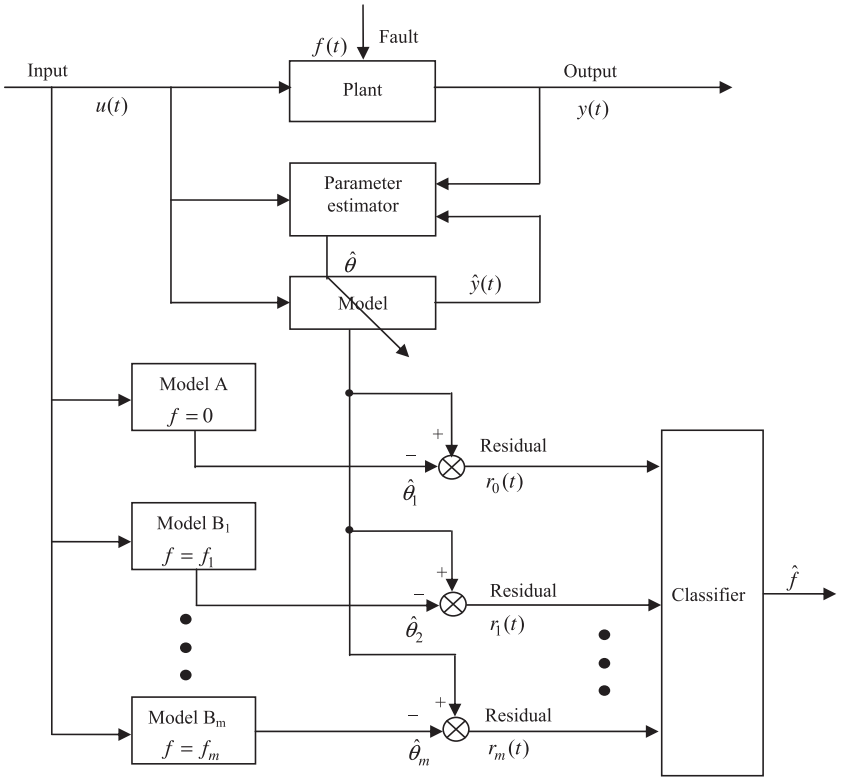

Fig. 2. Residual generation from parameter estimation.

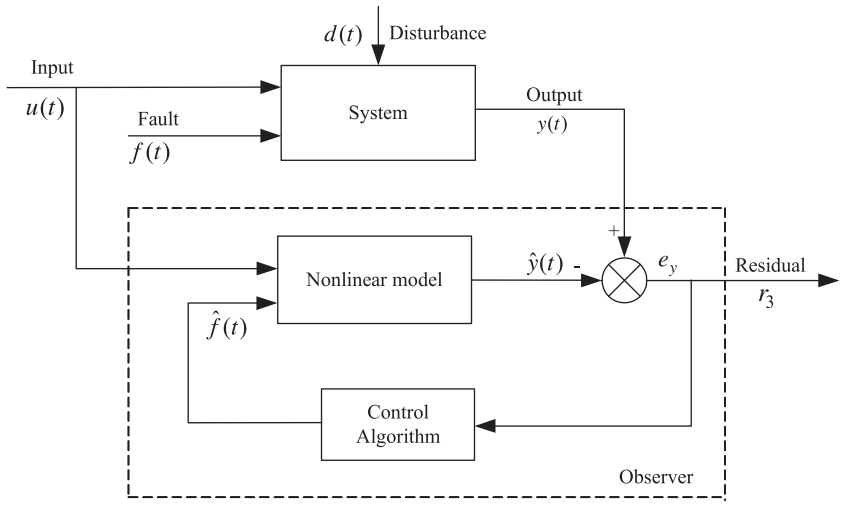

Fig. 3. Structure of residual signal generation.

in [16]. Sensor fault detection can be realized by the combination of statistical residual evaluation and fractal correlation dimension algorithm [45]. Evaluating the performance of fault diagnosis protocols applied to air-cooled unitary air-conditioning equipment is discussed in [46]. Energy efficiency involved fault detection in air-conditioning system and buildings are demonstrated in [47].

In this paper, a fuzzy relational sliding mode observer (FRSMO) is proposed to estimate the magnitude of slowly evolving faults in information-poor and non-linear systems. The performance of the proposed methods is evaluated using a cooling-coil subsystem of an air-conditioning plant in a simulated environment. The simulation results of the actuator fault and flow reduction fault estimation confirm the effectiveness of the proposed methods.

The remainder of the paper is organized as follows. The design of the neuro-fuzzy sliding mode observer for fault estimation is described in Section 2. A two-stage approach for model on-line adaptation is presented to reduce the effect of modelling errors on the fault estimates as well. Estimation of air-side fouling fault in a cooling coil subsystem of HVAC equipment is exemplified in Section 3. Section 4 discusses the sensitivity for the selection of dependent parameters in the neuro-fuzzy sliding mode observer fault estimation scheme. Effect of modelling errors in the fault estimation scheme is also described. The results of the long-term performance of the fault estimation scheme is presented and discussed in the same section. Conclusions are given in Section 5.

2. Neuro-fuzzy sliding mode observer

2.1. Problem formulation

2.1.1. Fuzzy relational model identification

Consider a general nonlinear dynamic system:

$$\begin{aligned} \dot{x}(t) &= G(x(t), u(t), d(t), f(t)) \\ y(t) &= H(x(t), u(t), f(t)) \end{aligned} \tag{2}$$

where $x \in R^n$ is the state variables, $u \in R^q$ $(q \le n)$ is the control signal and d is the disturbance; $y \in R^m$ is the output $(m \le q)$; $f \in R^p$ $(p \le m)$ is the fault vector; $G(\cdot)$ and $H(\cdot)$ are both smooth vector functions, which represent the relationship between the inputs, the faults and the outputs. A nonlinear multi-output system such as described in Eq. (2) can always be divided into several multi-input and single-output (MISO) subsystems, consisting n inputs $(x_1, x_2, \ldots, x_n)$ and one output y, where the input and output spaces are characterized by $r_1, r_2, \ldots, r_n$ and j fuzzy reference sets, respectively. Fuzzy relational model [48] is one of the modelling techniques that are applicable to these types of subsystems. The fuzzy relational model (FRM) can be described with the following fuzzy relational equation:

$$Y(k) = R \circ (X_1(k-1) \circ X_2(k-1) \circ \cdots \circ X_n(k-1)) \tag{3}$$

where $Y(k)$ is the present fuzzified crisp value of the controlled variable. The variables in the parenthesis on the right side are the previous fuzzified values of the manipulated $(x_1 = u)$ and controlled variables $(x_2, x_3, \ldots, x_n)$, R is the fuzzy relational array and "$\circ$" denotes fuzzy compositional inference. The elements of the rule confidence, $R_{r_1 r_2 \cdots r_n, j}$, indicates the amount of confidence of the output $y(k)$ when inputs are $x_{1,s_1}, x_{2,s_2}, \ldots, x_{n,s_n}$ $(1 \le s_1 \le r_1, 1 \le s_2 \le r_2, \ldots, 1 \le s_n \le r_n)$. The fuzzy relational model consists of $l(= r_1 \times r_2 \times \cdots \times r_n \times j)$ number of fuzzy rules. In building a FRM process, M and N are selected, the manipulated and controlled variables are first specified, and the number of fuzzy sets and fuzzy membership function are determined, including inference operation and identification algorithm. The final step is the defuzzification process and the crisp value of the output y can be obtained. The complete FRM is to find an array, R, containing the relationship of all the combination between inputs and output. The *global recursive least squares* (GRLS) algorithm is used to estimate the rule confidences R, and the element of R is calculated with $\hat{\theta}(t)$ vector:

$$\begin{aligned} \hat{\theta}(t) &= \hat{\theta}(t-1) + L(t)[y(t) - \varphi^T(t)\hat{\theta}(t-1)] \\ L(t) &= \frac{P(t-1)\varphi(t)}{\lambda(t) + \varphi^T(t)P(t-1)\varphi(t)} \\ P(t) &= \frac{1}{\lambda(t)}\left[P(t-1) - \frac{P(t-1)\varphi(t)\varphi^T(t)P(t-1)}{\lambda(t) + \varphi^T(t)P(t-1)\varphi(t)}\right] \end{aligned} \tag{4}$$

If one of the state $X_i(k)$ is regarded as the output of the model and the rest of the inputs are included in the second part, then the predicted fuzzy output from a FRM described in system (2) can be rewritten as:

$$\begin{aligned} \tilde{X}(k+1) &= R_1\tilde{X}_1(k) + R_2\tilde{X}_2(k) \\ Y(k+1) &= C\tilde{X}(k) \end{aligned} \tag{5}$$

where it predicts the fuzzy system output Y_{k+1} using the current input signal $[\tilde{X}_{1k}, \tilde{X}_{2k}]$ and its composition with the relational matrix $R = [R_1, R_2]'$; C is the unit output matrix. The estimated fuzzy output value Y_{k+1} is defuzzfied to its numerical value y_{k+1} by certain method, i.e., height or gravity-centre. With the aid of

reconstruction filter, the discrete-time output signal y_k from the model can be reconstructed into a continuous output signal y.

2.1.2. Sliding mode observer (SMO)

Originally the sliding mode observer is designed for a linear system subject to certain faults, which is given by

$$\begin{aligned}\dot{x}(t) &= Ax(t) + Bu(t) + Df_i(t)\\ y(t) &= Cx(t) + f_o(t)\end{aligned} \tag{6}$$

where $x(k) \in R^n$, $u(t)$, $y(t) \in R^m$ are state, control and output variables; A, B and C are relevant coefficient matrixes; f_i, f_o represent actuator and sensor fault, respectively. The objective is to design an observer to generate the state estimate $\hat{x}(t)$ and the output estimate $\hat{y}(t) = C\hat{x}(t)$ such that the sliding mode is reached and maintained where the output error

$$e_y(t) = \hat{y}(t) - y(t) \tag{7}$$

is forced to zero in a finite time. A particular sliding mode observer structure can be written in the form:

$$\dot{\hat{x}}(t) = A\hat{x}(t) + Bu(t) - G_l e_y(t) + G_n v \tag{8}$$

where G_l, G_n are appropriate gain matrices and v delegates a discontinuous component to keep the sliding mode movement. The estimate of the fault f_i, f_o can be computed from the equivalent output injection signal v_{eq} required to maintain sliding motion. The detailed design process can be referred in [16].

2.2. Fuzzy relational sliding mode observer for fault estimation

A fuzzy relational sliding model observer (FRSMO) is introduced to estimate the magnitude of a fault in a nonlinear system as described in system (2) including fault signals. The fault can be a sensor fault, actuator fault or component fault. As explained in Section 2.1, the output of the system in Eq. (2) can be computed from the structure of a fuzzy relational model in Eq. (5). When there is a fault, the input X is expressed as,

$$X = U \circ X_1 \circ X_2 \circ \cdots \circ X_n \circ F \tag{9}$$

where F is a fuzzified scalar system fault f. If it is the actuator fault, the fault f is part of the control signal, i.e., $u = u_0 + f$, where u_0 is the normal control signal. Then the input in Eq. (9) can be represented in Eq. (3). If it is a component fault or a sensor fault, the fault f can be represented as part of the input, i.e., $x_i = x_{i0} + f$ or an independent input x_i, where x_{i0} is the normal input value. So does the input described in Eq. (9) works in Eq. (3). A fuzzy relational sliding mode observer (FRSMO) is designed as

$$\begin{aligned}\dot{\hat{\tilde{x}}} &= R_1\hat{\tilde{x}}_1 + R_2\tilde{x}_2 + G_l e_y + G_n v\\ \hat{y} &= C\hat{\tilde{x}}\end{aligned} \tag{10}$$

where G_l and G_n are appropriate gain matrices, $e_y = (y - \hat{y})$ is the output estimation error and v represents a discontinuous switched component to induce a sliding motion. The matrix G_l is designed to guarantee the stability of the system. Since the designed observer system is inherited stable (bounded with the output from fuzzy relational model), here, $G_l = 0$. The observer input $G_n v \in R$ is designed to estimate the fault, when the system obtains and arrives at the $e_y = 0$ and $\dot{e}_y = 0$. Since, when the state error is defined as $e_x = \tilde{x} - \hat{\tilde{x}}$, here $e_x = e_y$, it follows $e_x \to 0$ and the error function $\dot{e}_x$ becomes

$$0 = R_1 e_x - Df + v_{eq} \tag{11}$$

where v_{eq} is the so-called equivalent output injection signal. The equivalent output injection represents the average behaviours of the discontinuous component v and represents the effort necessary to maintain the motion on the sliding surface. Once the sliding motion is attained, then

$$v_{eq} \to Df \tag{12}$$

The order of the motion equation in this type of sliding mode is equal to the dimension of the sate space [49]. The switching function S is designed as the combination of the output error e_y,

$$S = c_1 e_y + c_2 \dot{e}_y \tag{13}$$

where c_1 and c_2 are positive scalars. It can be shown that once a sliding motion is attained, estimate of the fault can be computed from the *equivalent output injection* signal required to maintain sliding motion. The discontinuous vector v is defined by

$$v = \begin{cases} -\rho ||D|| \dfrac{Pe_y}{||Pe_y||} & \text{if } e_y \neq 0\\ 0 \end{cases} \tag{14}$$

where D is the fault matrix; P is the rectification matrix to make sure observer stable as well; the positive scalar ρ is chosen so that $||f(t)|| < \rho$. One way to recover the equivalent output injection signal is to use the low-pass filter, i.e., fault estimation filter (FEF), to get the estimated fault $\hat{f}$,

$$\hat{f} = (D^T D)^{-1}(D^T D)D^{-1} v_{eq} \frac{1}{(\tau_f s + 1)^q} \tag{15}$$

where τ_f is the time constant, which is selected based on the fault characteristics.

The general structure of an observer-based fuzzy sliding fault estimation scheme is shown in Fig. 4. The nonlinear plant is described by the fuzzy relational model. The control and other input are delegated by X, and f is the additive fault, which can be an actuator fault or a sensor fault. It should be noted that fuzzy relational models are discrete-time models. Therefore, additional factors, such as modelling errors and reconstruction filter must be considered in the design of the fault estimation scheme. After the reconstruct filter (*RF*), the discrete-time signal output from FRM, $\hat{y}_d$, is reconstructed in a continuous-time form, $\hat{y}$, which is compared to the actual measurement from the system, y, thus obtaining the output error e_y. The output error signal is used for the sliding mode surface construction and sliding mode motion.

In the paper, fuzzy relational model is adopted for the system behaviour description instead of linearization methods or other fuzzy approaches. Wu and Saif designed a neural-fuzzy sliding mode observer for fault diagnosis [43], in which a T-S fuzzy system is used for the system description. The advantage of the T-S model is that it has few rules compared to other neural fuzzy model. However, T-S fuzzy model is composed of several linear subsystems with nonlinear dependence and there is no theory for the premise parameter selection in the process [37,50]. Besides, the accuracy of the output from the model has to be improved via increasing number of inputs or number of parameters. The parameters have also to be updated online with adaptive model to accommodate the parameters to cover all circumstances if the regions cannot be represented with required quality. As for fuzzy relational model, the system behaviour can be described with the rule array with no region partition in the state-space, which would result in certain system errors.

Three filters are used in the scheme (shown Fig. 4). The fault estimation filter (*FEF*) has already been discussed above. A reconstruction filter (*RF*) is added to the system to recover the continuous-time output signal from the discrete-time fuzzy relational model. An anti-aliasing filter (*AaF*) in the SMO scheme is used to remove high frequency component of v, which could cause aliasing problems during sampling. When a signal is not sampled at a

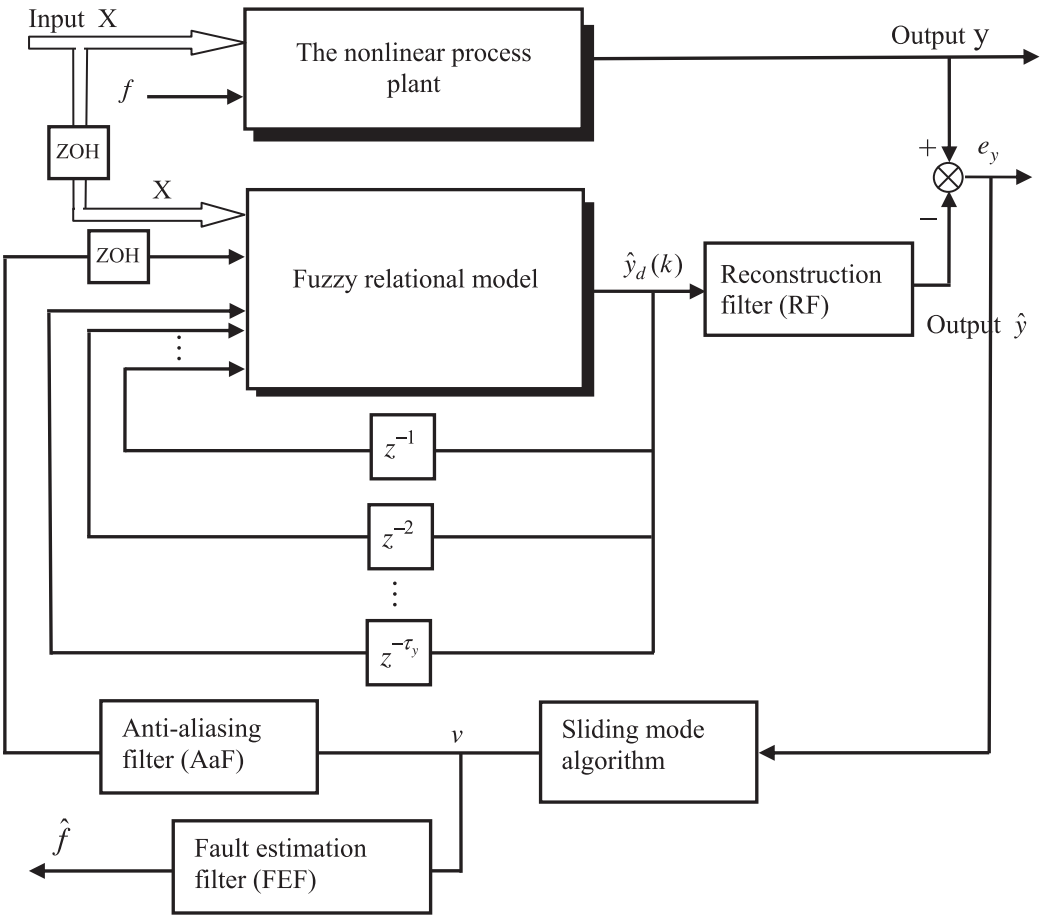

Fig. 4. Fuzzy relational sliding mode observer.

high enough rate, i.e., below the Nyquist Frequency, the problem of aliasing occurs, which will cause the original high frequencies in the signal to fold back into lower frequencies and produce highly undesirable artefacts in the reconstructed signal. The anti-aliasing filter restricts the bandwidth of the signal before it is sampled. Because the signal from the FRSMO is a high frequency switching signal, an anti-aliasing filter is used to filter the signal to ensure the applicability of the passed signal. Here, the anti-aliasing filter (*AaF*) is a first-order or second-order low-pass filter,

$$G(s)_{AaF} = \frac{1}{\tau_a s + 1} \quad \text{or} \quad G(s)_{AaF} = \frac{1}{(\tau_a s + 1)^2} \tag{16}$$

where τ_a is the time constant of the filter. The selection of the time constant of *AaF* depends on the sampling time and the characteristic of the system.

2.3. A two-stage approach for on-line adaptation

2.3.1. Description of the on-line fault estimation scheme

The incipient fault is diagnosed by the fuzzy relational model and sliding mode observer. The initial fuzzy relational model considers the actuator fault in the modelling process. As for sensor fault, however, in is not included in the initial stage. Once the fault evolves large enough and the faulty system will not be described by the initial model, model update is necessary to be used during the fault diagnosis process so that system behaviour can be captured accurately. Consider the nonlinear system described in Eq. (2) can be rewritten as,

$$\begin{aligned} \dot{x} &= G(x, u, \theta_s, f) \\ y &= H(x, u, \theta_s) \end{aligned} \tag{17}$$

where $x \in R^n$ represents the vector of the state variables; $u \in R^r$ is the input ($r \le n$); $\theta_s \in R^k$ is the parameter vector of the model; $y \in R^m$ is the output vector of the model ($m \le n$). f is the actuator or component fault of an unknown nature with p dimensions ($p \le m$). It is assumed that $G(\cdot)$ and $H(\cdot)$ are analytical functions. A model of the system can be assumed to be of the form:

$$\begin{aligned} \dot{\hat{x}} &= \hat{G}(\hat{x}, u, \hat{\theta}_s, \hat{f}) \\ \hat{y} &= \hat{H}(\hat{x}, u, \hat{\theta}_s) \end{aligned} \tag{18}$$

where $\hat{x}$ is the estimated state, $\hat{\theta}_s$ is the estimated parameter vector, $\hat{y}$ is the estimated output and $\hat{f}$ is the estimated fault, $\hat{G}(\cdot)$ and $\hat{H}(\cdot)$ are analytical functions. Once a fault occurs in the system, the parameters of the model $\hat{\theta}_s$ will diverge from their true values θ_s. Therefore, the reliability of the fault diagnosis system cannot be guaranteed. To overcome this problem, both parameter estimation and fault estimation can be performed over different time intervals [51]. There are two stages in the scheme, model identification (MI) and fault estimation (FE). The scheme starts with a MI stage. If the fault develops slowly, the fault estimation can take place more often than parameter estimation. The values of the parameters are assumed to stay constant during the FE stage, while the fault is assumed to be constant during the MI stage.

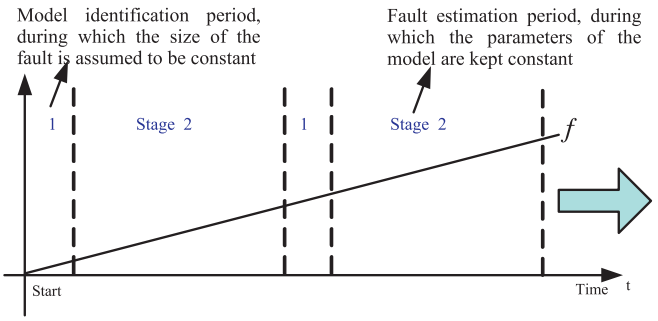

Fig. 5. On-line learning scheme for model update and fault estimation.

The two-stage process is illustrated in Fig. 5, where stage 1 and stage 2 are repeated alternately. The optimal interval between the two stages will depend on the nature of the fault and variations in the parameter vector as well. However, in general parameter estimation is only performed periodically but infrequently over a short period of time, so that the fault can be identified for the vast majority of the time.

A global least square algorithm is used to adjust the model parameters in the on-line learning fault estimation scheme (OLFES). A fuzzy relational sliding mode observer (FRSMO) is used to estimate the magnitude of the fault.

2.3.2. Overview of the on-line learning fault estimation scheme

The system output expressed in Eq. (2) can be rewritten as:

$$y = \Phi\left(\theta_s, u, v_0, f, t\right) \tag{19}$$

where θ_s is the parameter vector of the system, u is a control signal, y is the output, t is the time, v_0 is the vector of the initial conditions of the system, and f is the fault signal. The function $\Phi(\cdot)$ captures the relationship between input, output and fault. Let the model be of the following form,

$$\hat{y}_M = \hat{\Phi}(\hat{\theta}_M, u, v_0, \hat{f}, t) \tag{20}$$

where $\hat{\theta}_M$ is the parameter vector of the model, $\hat{y}_M$ is the output from the model and $\hat{f}$ is the estimate of the fault; $\hat{\Phi}$ is the function to describe the relationship between input, output and fault. The initial model is updated on-line when the scheme starts to perform to make sure that the model is the correct description of current system behaviour. After the completion of the first MI stage, the model becomes

$$\hat{y}'_M = \hat{\Phi}(\hat{\theta}^1_M, u, v_0, \hat{f}^1, t) \tag{21}$$

where $\hat{\theta}^1_M$ is the updated parameter vector and $\hat{y}'_M$ is the model output. It is supposed that the plant is initially fault-free and the initial estimate of the fault is zero. If it is assumed that the kth MI is ideal and $\Phi = \hat{\Phi}$, then $\hat{y}^k_M = y$, $\hat{\Phi}(\hat{\theta}^k_M, u, v_0, 0, t) = \Phi(\theta_s, u, v_0, 0, t)$, and

$$\hat{\theta}^k_M = \theta_s, \tag{22}$$

if it is also assumed that at the kth stage, the FE is ideal, then $\hat{f}^k = f$ and

$$\hat{y}'_{M_k} = y, \tag{23}$$

$$\therefore \quad \hat{\Phi}(\hat{\theta}^k_M, u, \hat{f}^k_M, t) = \Phi(\theta_s, u, f, t), \tag{24}$$

where $\hat{f}^k_M$ is the final value of the estimated fault after the completion of the kth FE stage.

The fault estimation (FE) is accomplished via the method described in Section 2.2 (as shown in Fig. 4), which is followed by MI stage. Hence, the one periodical phase of the FE and MI processes (the on-line fault estimation scheme) is depicted in Fig. 6. The value of the $\hat{f}_M$, which is taken from the result of the previous stage of FE, is used for the next $(k+1)$th model update. After performing the scheme several times, $\hat{\theta}^k_M$ should gradually come close to θ_s and $\hat{f}$ should converge to the actual fault f with bounded error.

3. Example application: flow reduction caused by air-side fouling in a cooling coil

3.1. Introduction of HVAC system and a cooling-coil subsystem

It is difficult to test a fault estimation experiment in a real application environment, especially for the incipient faults. For abrupt faults, it is not possible to perform destructive testing under normal operating conditions. For incipient faults, it takes too long to wait for the fault growing to the alarm threshold. Simulation experiment is a good alternative to test the fault estimation scheme.

In offices and other commercial buildings, centralized HVAC Variable Air Volume (VAV) air-conditioning systems are often used

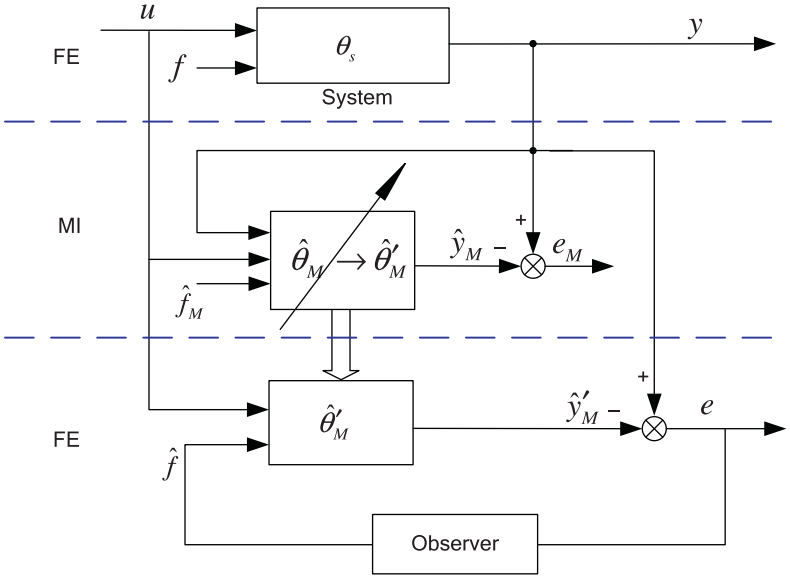

Fig. 6. Diagram of the online learning fault estimation scheme.

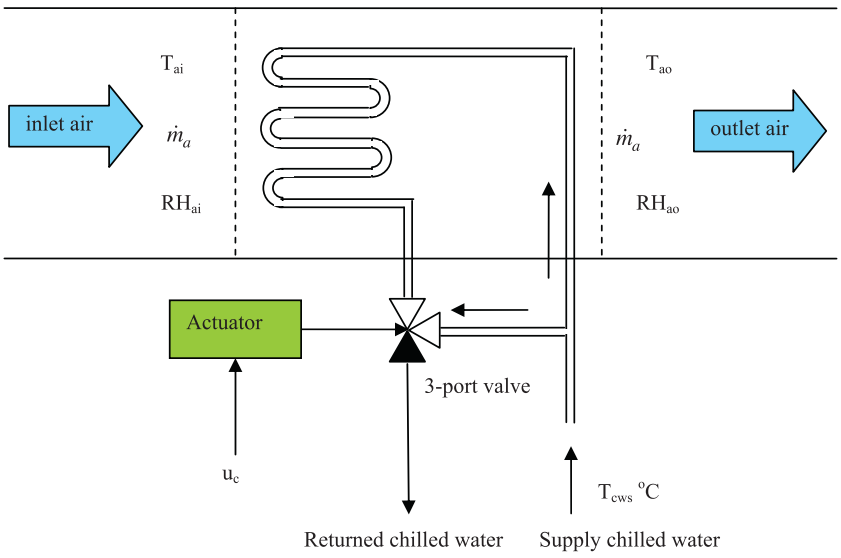

Fig. 7. Schematic diagram of the cooling coil subsystem.

to adjust the indoor thermal environment through a duct network. An Air Handling Unit (AHU) is used to control the air condition and usually comprises of a section to mix outside and recirculated air from the conditioned space, heating and cooling coils, a humidifier and supply and extractor fans.

The cooling coil subsystem consists of an actuator, a three-port control valve, a supply air temperature sensor and a cooling coil. A schematic diagram of the cooling coil subsystem is shown in Fig. 7 [60]. The chilled water supply, at temperature T_{cws} °C, is pumped through the copper tubes of the cooling coil. Inlet air temperature at T_{ai} °C with air relative humidity RH_{ai}% and air mass flow rate $\dot{m}_a$ kg s^{-1} is passed over the copper tubes. Cooled outlet air at temperature T_{ao} °C with air relative humidity RH_{ao}% leaves the cooling coil. The water flow rate through the coil is varied by a 3-port mixing-valve. The position of the valve actuator is determined by a control signal u_c, where in the range $0 \le u_c \le 10$ V.

Collecting complete data from a real system is difficult since the model needs to be trained under all possible operating conditions and this would be a time consuming process. Computer simulation is therefore used here. The simulation is based on a software package known as SIMBAD (Simulator of Building And Devices) which was developed to set up the models of components and plants for the design and testing of HVAC systems [52]. Nine different designs of cooling coil have been developed by the control group at Oxford University [53]. The parameters and detailed coil data for the nine cooling coil subsystems can be refereed in [54].

3.2. Modelling the cooling-coil subsystem

Based on the physical theory and the control point of view, the Fuzzy Relational Model (FRM) of the cooling coil subsystem (D1) has five inputs and one output and the model structure is shown in Fig. 8. The values of the input and output are normalized to lie in the range [0,1] before the training takes place [55].

The FRM is equivalent to a second-order dynamic system. The sampling time of the FRM is set to 10 s as the dominant time constant of the cooling coil is of the order of 100 s. The estimated outlet air temperature $T'_{ao}(n)$ is given by the following fuzzy relation:

$$T'_{ao}(n) = R \circ U(n-1) \circ \dot{m}_a(n-1) \circ T'_{ao}(n-1) \circ T'_{ao}(n-2) \qquad (25)$$

where R is the fuzzy relational matrix representing the relationship between the input and output variables; $U(n-1)$ is the normalized actuator control signal at the $(n-1)$th sample time; $T'_{ao}(n-2)$, $T'_{ao}(n-1)$ and $T'_{ao}(n)$ are the previous and current normalized outlet air temperatures; $\circ$ denotes fuzzy compositional inference. $\dot{m}_a$ is the reduced air flow rate, $\dot{m}_a(n-1) = \dot{m}_{aD}(n-1) - f_{\dot{m}_a}(n-1)$ and $f_{\dot{m}_a}$ is a small reduction in $\dot{m}_{aD}$ caused by the fouling. For simplicity, the variation of the inlet air temperature T_{ai} is held constant and the temperature of the chilled water supply T_{cws} is also assumed constant during these experiments.

The relationship between the control signal U and outlet air temperature T_{ao} is nonlinear. The T_{ao} is more sensitive to the control signal when the valve moves from a fully closed to a half open position than from a half open to a fully open position. The partition of the control signal in fuzzy reference space is therefore non-uniform, and there are more partitions in the first part of the reference space [54,56].

The values of the outlet air temperature $T_{ao}(n-2)$, $T_{ao}(n-1)$ and $T_{ao}(n)$ are assumed to be from 12 °C to 30 °C so that the model can deal with the full range of outlet air temperatures that occur in an air-conditioning system. Five equally-spaced fuzzy sets are defined over the universes of discourse. For simplicity, two fuzzy reference sets are chosen for the current outlet air temperature $T_{ao}(n)$, without loss of generality. Here, it is an example of a nonlinear system to be applied for the experiments of the incipient fault estimation. If the system is described in a liner form, it is a simplified model with little dynamic information. Besides, not all systems can be linearized. In this case, more parameters are used to increase the accuracy of the predicted model. In engineering practice, the number of the parameters can be reduced under certain situations.

An incipient fault of flow reduction caused by air-side fouling in the cooling coil subsystem of an air-conditioning system is

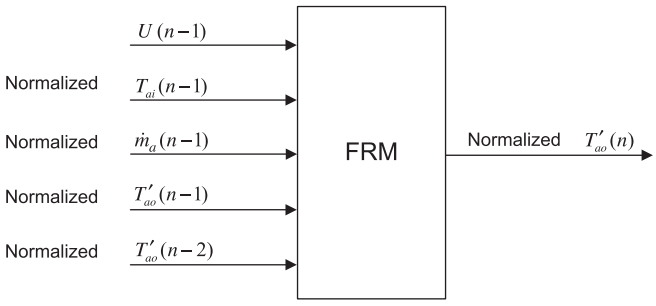

Fig. 8. Structure of the air-side fouling fault model.

Table 1
Sliding mode surface settings for an incipient fault estimation using SMO and a discrete-time model.

Parameter settings			
Control signal	Sliding surface	$G(s)_{AaF}$	$G(s)_{FEF}$
$u_a = 0.3$	$S = 500\dot{e} + e, \quad M = 0.5$	$\frac{1}{200s+1}$	$\frac{1}{(3600s+1)^2}$

identified with the FRSMO fault estimation scheme. Flow reduction $f_{\dot{m}_a}$ has been found to increase during the operation of the plant so that the air flow rate drops by 20% over a period of two years [57]. In this application, the capacity of the air flow rate is assumed to decrease by 12% after one year to reduce the calculation burden.

4. Results of FRSMO fault estimation scheme

4.1. Parameter selection in FRSMO

FRSMO estimation scheme has been introduced in Section 2. It should be noted that there is no systematic pattern to be followed for the parameter selection. A series of simulation experiments are conducted to investigate the selection of the parameters in the fault estimation schemes. An ideal model of the system is used for the following simulation tests to avoid the effects of modelling errors in the results. The parameter selection for the two filters, *AaF*, *FEF* and sliding mode surface are discussed as follows.

A second-order Hammerstein model of a non-linear dynamic system [58] which is a simplified version used to discuss the parameter selection in fault estimation. The relationship between the control signal $u(t)$ and the output $y(t)$ of the cooling-coil subsystem described in Fig. 7 can be expressed in the simplified Laplace-transform form as,

$$y(s) = L(q(u(t))) \cdot G(s)$$
$$\text{where} \quad G(s) = \frac{1}{(1+\tau s)^2} \tag{26}$$

where $\tau = 120$ s is the time constant. The nonlinear function $q(\cdot)$ describes the static behaviour of the control signal. Here, it is given by,

$$q(u) = \frac{1}{3.433} \ln(30u + 1) \tag{27}$$

The observer scheme depicted in Fig. 4 is used in the following tests. Suppose there is only one fault acting on the system.

4.1.1. Sliding mode surface design

The ideal discrete-time model of the system described in (26) is given by,

$$y(z) = q(u)G(z) = q(u) \cdot \frac{0.003285z + 0.003108}{z^2 - 1.8401z + 0.8465} \tag{28}$$

where $G(z)$ is the Z-Transformation of $G(s)$. The sampling time in the discrete-time model is 10 s. The general test environments are given in Table 1, which is set based on the industrial experience knowledge and perfect model of the system. The rate of change of the fault is 1×10^{-6} and the simulation time is 10,000 s.

The results of fault estimation using a SMO with four different sliding surfaces are shown in Fig. 9. The two values in the brackets denote the value of the c_1 and c_2, where the sliding surface S is given by,

$$S = c_1\dot{e} + c_2 e \tag{29}$$

The switching function of the sliding mode surface is constructed by the intersection of some hyper surfaces in the state space. Based on the estimated results, the design S_2 is more suitable in this application.

Table 2
The designs of *AaF*.

Anti-aliasing filters in Fig. 11			
$G(s)_{AaF1}$	$G(s)_{AaF2}$	$G(s)_{AaF3}$	$G(s)_{AaF4}$
$\frac{1}{400s+1}$	$\frac{1}{300s+1}$	$\frac{1}{200s+1}$	$\frac{1}{100s+1}$

The fault estimates with different values of the gain M are shown in Fig. 10. The gain must be chosen to ensure the movement to reach and maintain on the sliding surface. However, the value can also affect the size of the limited cycle [59]. Therefore, there is a trade-off between the system response speed and accuracy of the fault estimate. It can be shown that M_3 is more appropriate in this case.

4.1.2. The AaF design

The estimation results with different anti-aliasing filters are shown in Fig. 11. The designs of *AaF* (Table 2) used to generate the results are as follows.

It can be seen that the results are strongly dependent on the design of the *AaF* (see Section 2.2) to acquire the signal to match the system behaviour. Fig. 11 shows the fault estimates with different fault estimation filters. As there is no known automatic technique to be applied to select the parameters of the FRSMO, trial and error must be used to test the effect of different values of the parameters of the filter.

4.1.3. The FEF design

The *FEF* designs (Table 3) used to generate the results in Fig. 12 are as follows.

The filter with a small time constant cannot remove the high frequency part of the signal; whereas the filter with a large time constant has an adverse effect on the response of the fault estimator. The offset between the fault estimate and the actual fault would be enlarged due to the phase lag in the filter. A convenient trade off must be found between the reliability and estimate accuracy. Considering the fault characteristics, FEF_3 is the best selection in the fault estimate scheme.

4.1.4. Robustness of the fault estimate scheme

The results of the fault estimation using a sliding mode observer for two different rates of change of the actual fault are shown in Fig. 13. The rate of change of f_1 is 1×10^{-6} and that is 0.2×10^{-6} of f_2. The two tests are under the same parameter settings. The errors between the actual and estimated fault from the simulation are $\Delta f_{1test} = 5.8589 \times 10^{-4}$ and $\Delta f_{2test} = 5.8872 \times 10^{-5}$. Once again, the results confirm the robustness of the sliding mode observer estimation scheme.

The fault estimation scheme of the SMO in a nonlinear system with a discrete-time model $(M)_d$ is discussed. The sensitivity of the fault estimate to several aspects of schemes is summarized in Table 4.

In summary, the preliminary selection of the parameters in FRSMO is based on the human experience. In simulation application, perfect model of the system can greatly enhance the availability of the selections of the parameters in the scheme. Trial

Table 3
The FEF design.

Fault estimation filters in Fig. 12			
$G(s)_{FEF1}$	$G(s)_{FEF2}$	$G(s)_{FEF3}$	$G(s)_{FEF4}$
$\frac{1}{(1200s+1)^2}$	$\frac{1}{(2400s+1)^2}$	$\frac{1}{(3600s+1)^2}$	$\frac{1}{(6000s+1)^2}$

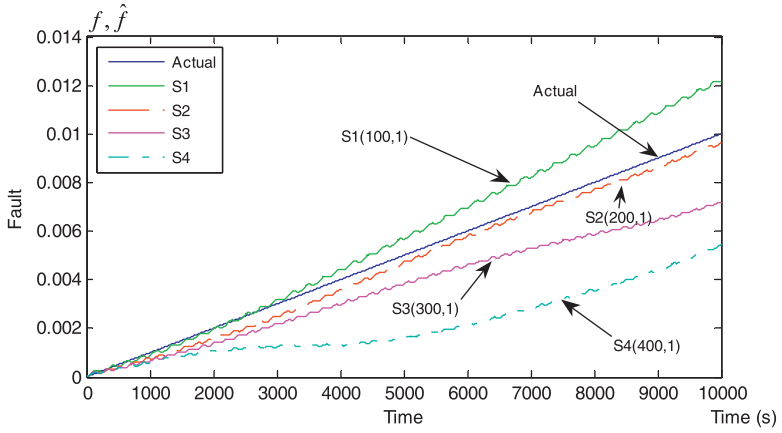

Fig. 9. The effect of the sliding surface on the fault estimate using a SMO.

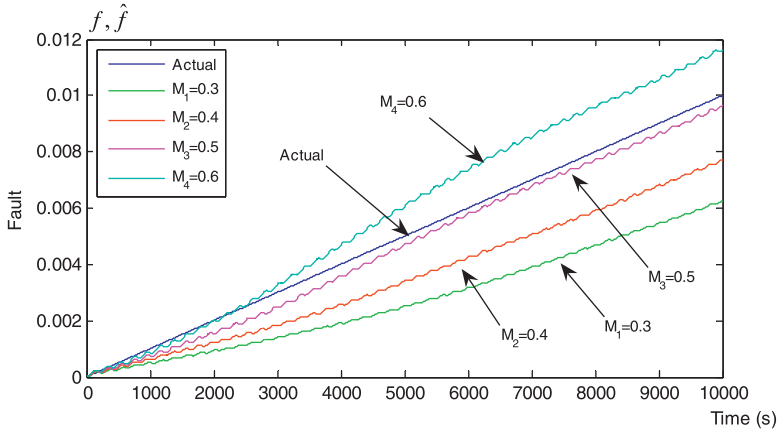

Fig. 10. The effect of gain M on the fault estimate using a SMO.

Table 4
Sensitivity of the two fault estimation schemes.

	Parameter settings	Rate of change of the fault	Value of the control signal	Anti-aliasing filter	Fault estimation filter
SMO & $(M)_d$	No	No	Yes	Yes	Yes

and error method is necessary to be applied to adjust the values of the parameters in the fault estimation scheme based on certain controlled systems.

4.2. Effects of the modelling errors in the fault estimation scheme

The desired value of the outlet air temperature T_{aoD} changes between 12 and 30 °C, which is assumed as the disturbance in the system. Two of the designs D1 and D3 of the cooling coil subsystem are selected for fault estimation experiments, where there are nine designs for the cooling coil subsystems which are developed in control group, Oxford University. Results of the fault estimate from two models are presented to investigate the influence of modelling errors. The first type of the experiment uses **Model A**, which is trained off-line using the correct design (D1). It means that this

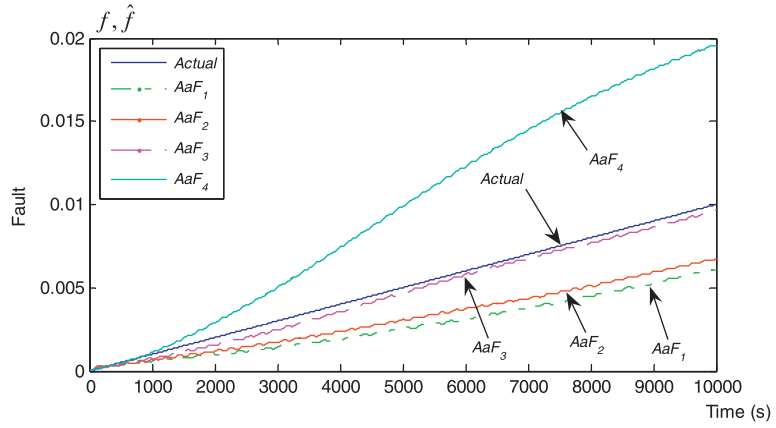

Fig. 11. The effect of anti-aliasing filter on the fault estimates using a SMO.

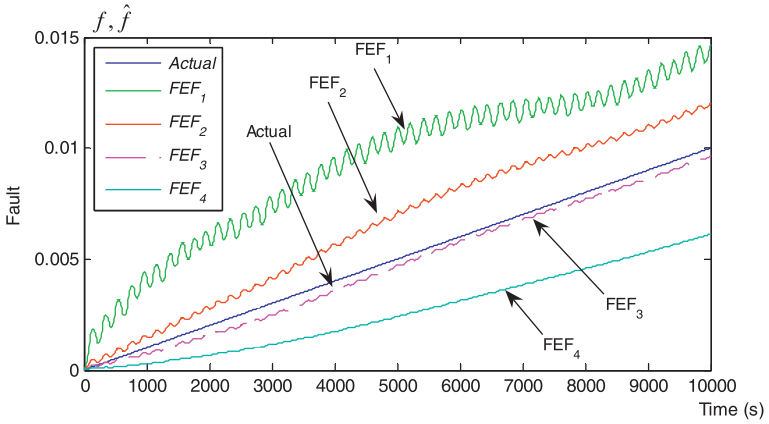

Fig. 12. The effect of fault estimation filter on the fault estimates using a SMO.

model is trained using the data generated from the same system which is used for testing the fault identification scheme. The second type of the experiment uses **Model B**, which comprises a model that is trained off-line using a cooling coil design (D1) that is different from the simulated cooling coil design (D3) used for fault identification. It is assumed that **Model B** has modelling errors and it is not the ideal model of the plant.

The results for long-term flow reduction fault estimation using the two models are shown in Fig. 14. It can be seen that there is a large offset between the actual and estimated fault when **Model B** is used and a small decreasing offset when **Model A** is used. It is reiterated that the introduction of **Model B** in the tests is to investigate the sensitivity of the modelling errors due to the practical difficulty in acquiring high quality of the model of the plant. The average offset between the fault estimates obtained from **Model A** and the actual fault is 0.03.

However, the average offset between the fault estimates obtained from **Model B** and the actual fault is 0.11. This is mainly caused by the modelling errors, which come from two sources. One is due to the discrepancy between the **Model B** and the simulated plant [54]. The other is due to the variation of the faulty behaviour in the system. The faulty air flow rate is one of the inputs in the model and **Model A** has only been trained (on-line) for very small range of fouling. Therefore, there exists the offset between the actual fault and the estimated fault from **Model A**. It is concluded that a on-line scheme must be developed to reduce modelling errors in the fault estimation.

4.3. Long-term flow reduction fault estimation using OLFES based on a FRSMO

A fault estimation scheme with on-line learning (OLFES) has been proposed in Section 2.2 to deal with the problems associated with modelling errors. The flow reduction in air-side fouling is also increased to 24% in two years. The parameter settings in the fuzzy relational sliding mode observer are as follows: the sliding surface (S) is $5\frac{de}{dt} + e$ and the gain (M) in the sliding controller is 0.5; the values of the switch on/off point in the relay are ± 0.001; the output of the relay are ± 0.5.

Two stages of the model update and fault identification are performed alternatively in the procedure. During the MI stages, the parameters of the model are updated on-line by the new measurements. In the mean time, the fault estimates are obtained from the fault identification programme with the original model. After the completion of MI stage, the updated model is transferred to the FE stage which is used to estimate the fault. The parameters of the model are kept constant during the FE stages. Several experiments were performed to test the sensitivity of the fault estimates to different length in MI and FE stages. The performance of three schemes is investigated (see Table 5).

The results of fault estimates are shown in Fig. 15. Because the initial modelling errors are very large, there is a gradually decrease in the estimated results after the first MI update. The estimated fault in the first day is assumed as 0. The values of the RMSE of the estimated faults are listed in Table 6.

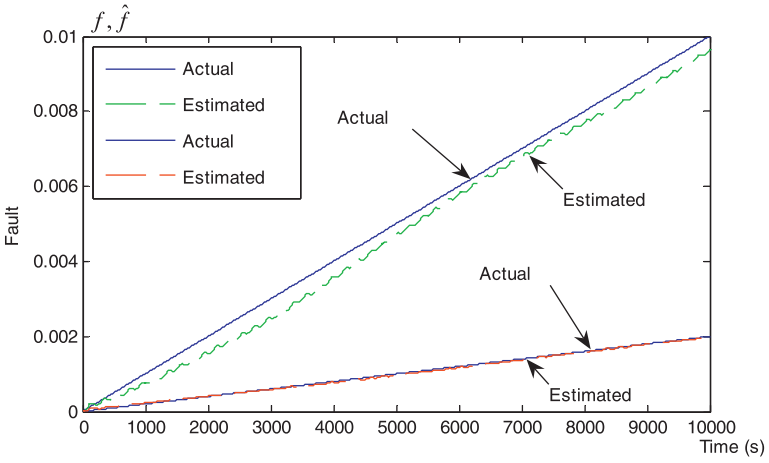

Fig. 13. Results of fault estimation using a SMO for different rates of the fault.

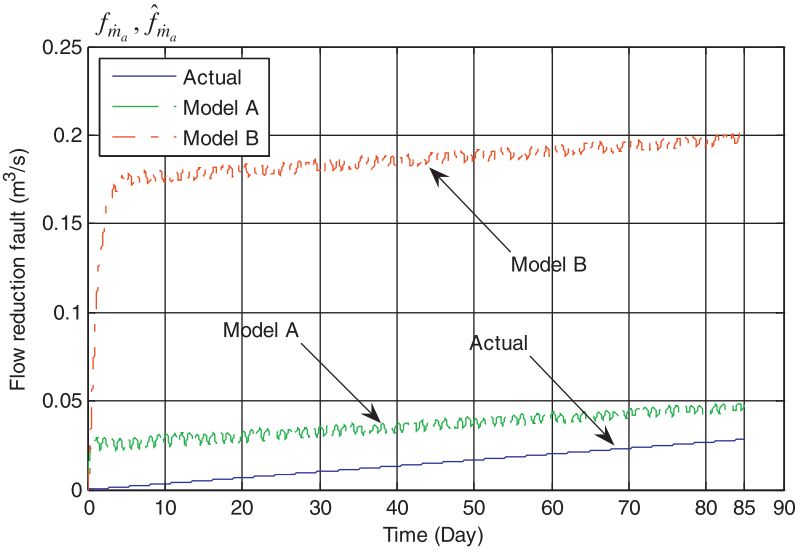

Fig. 14. Results of flow reduction fault estimation using two different models with SMO.

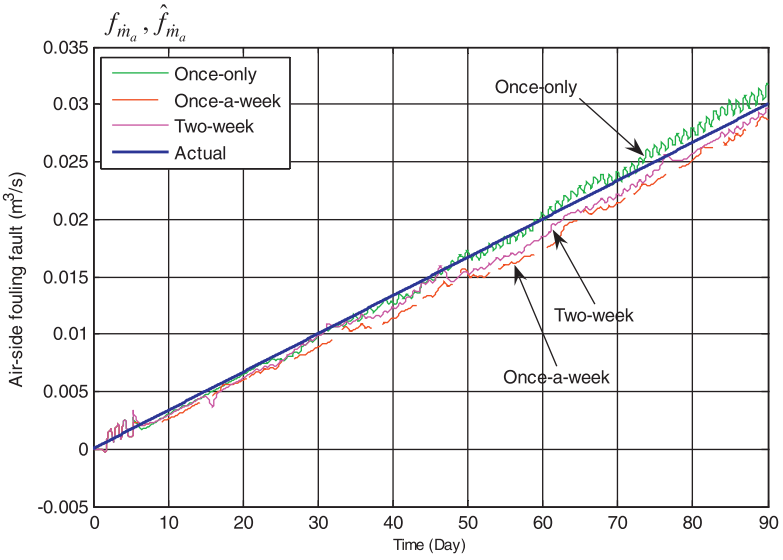

Fig. 15. Air-side fouling estimates with different time intervals in MI and FE stages using OLFES and a FRSMO.

When a SMO is used in the fault estimation scheme, there is no steady-state error in the estimated fault if the system reaches and is maintained on the sliding surface. However, this is unlikely to be achieved in nonlinear and discrete-time systems. Due to the nonlinearities of the system, an offset occurs when the system motion moves around the sliding surface and there will be a steady-state error. For discrete-time systems, the sampling interval makes the system move away from the sliding surface and back again. The movement results in a limit cycle which could also cause steady-state errors.

Table 5
Different time intervals used in the on-line fault estimation scheme.

No.	Scheme	MI	FE
1	Once-only	The first day	The rest of the time
2	One-a-week	1day	1 week
3	Two-week	1day	2 weeks

Table 6
RMSEs of the air-side fouling fault estimates with different time intervals.

	Once-only scheme	Once-a-week scheme	Two-week scheme
RMSE	0.0018	0.0013	0.0010

The estimated fault from the "once scheme" is reasonably good in the early stages. However, the short term fluctuations in the fault estimates gradually become larger because the model used for fault estimation needs to be updated as the size of the fault increases. The estimated fault is closer to the actual fault when the once-a-week scheme is used. However it can be seen that the RMSE derived from the two-week scheme has the smallest value. Therefore, longer time intervals between the MI stages and FE stages should be considered in the on-line learning fault estimation scheme.

5. Conclusions

General concepts of faults and methods of incipient fault estimation have been reviewed in the paper. A fuzzy relational sliding mode observer (FRSMO) has been developed to identify the incipient faults in nonlinear systems. Potential factors and the resulted

in estimation errors in the fault estimates have been discussed. A two stage, on-line learning, fault estimation scheme is proposed to update the model and reduce modelling errors due to the influence of fault on the system behaviour. The fuzzy relational sliding mode observer is used to estimate the incipient faults in the subsystem. Ideal model is used in the initial experiment settings so that there are only very small rounding errors in the discrete-time case. The SMO is rarely sensitive to the operating conditions and the rate of change of the fault.

A cooling coil subsystem is used as a case study to examine the effectiveness of the methods. Several model updates have to be performed for the flow reduction estimation. After the first model update, the fault estimate gradually converges to the actual value. The impact of modelling errors is greatly reduced in the on-line fault estimation schemes. The scheme has been shown to be robust and the convergence of the schemes can be assured in most conditions. The fault estimation in a cooling-coil subsystem has confirmed the effectiveness and reliability of the on-line FRSMO scheme.

References

[1] S. Simani, C. Fantuzzi, R. Patton, Model-Based Fault Diagnosis in Dynamic Systems Using Identification Techniques, Springer, London/New York, 2003.
[2] P.M. Frank, Fault diagnosis in dynamic systems using analytical and knowledge-based redundancy: a survey and some new results, Automatica 26 (3) (1990) 459–474.
[3] R.D. Montgomery, R. Baker, Study verifies coil cleaning saves energy, ASHRAE Journal 48 (11) (2006) 34–36.
[4] P.M. Frank, Analytical and qualitative model-based fault diagnosis – a survey and some new results, European Journal of Control 2 (1996) 6–28.
[5] P.M. Frank, S.X. Ding, T. Marcu, Model-based fault diagnosis in technical processes, Transactions of the Institute of Measurement and Control 22 (1) (2000) 57–101.
[6] P.M. Frank, X. Ding, Survey of robust residual generation and evaluation methods in observer-based fault detection systems, Journal of Process Control 7 (6) (1997) 403–424.
[7] J.J. Gertler, Survey of model-based failure detection and isolation in complex plants, IEEE Control Systems Magazine 8 (6) (1988) 3–11.
[8] R. Isermann, Model-based fault-detection and diagnosis – status and applications, Annual Reviews in Control 29 (1) (2005) 71–85.
[9] S.a.A.M. Leonhardt, Methods of fault diagnosis, Control Engineering Practice 5 (5) (1997) 683–692.
[10] R.J. Patton, R. Clark, P.M. Frank, Issues of Fault Diagnosis for Dynamic Systems, Springer-Verlag, 2000 London Limited, 2002, 3540199683.
[11] R. Patton, R. Clark, P.M. Frank, Issues of Fault Diagnosis for Dynamic Systems, Springer, London/New York, 2000.
[12] M.A. Demetriou, Using unknown input observers for robust adaptive fault detection in vector second-order systems, Mechanical Systems and Signal Processing 19 (2) (2005) 291–309.
[13] A.A. Stoorvogel, H.H. Niemann, P. Sannuti Saberi, Optimal fault signal estimation, International Journal of Robust and Nonlinear Control 12 (8) (2002) 697–727.
[14] A.L. Dexter, D. Ngo, Fault diagnosis in air-conditioning systems: a multi-step fuzzy model-based approach, HVAC and R Research 7 (1) (2001) 83–102.
[15] S.K. Spurgeon, Sliding mode observers: a survey, International Journal of Systems Science 39 (8) (2008) 751–764.
[16] C. Edwards, S.K. Spurgeon, R.J. Patton, Sliding mode observers for fault detection and isolation, Automatica 36 (2000) 541–553.
[17] C.P. Tan, C. Edwards, Sliding mode observers for detection and reconstruction of sensor faults, Automatica 38 (10) (2002) 1815–1821.
[18] C. Edwards, S.K. Spurgeon, Sliding Mode Control: Theory and Applications, CRC Press, 1998.
[19] X. Wen, H. Zhang, I. Zhou, Fault Diagnosis and Fault-tolerant Control for Control System, China Machine Press, 1998.
[20] A. Ray, R. Luck, An introduction to sensor signal validation in redundant measurement systems, IEEE Control Systems Magazine 11 (2) (1991) 44–49.
[21] G. Delmaire, J.P. Cassar, M. Staroswiecki, Comparison of identification and parity space approaches for failure detection in single input single output systems, in: Proceedings of the Third IEEE Conference on Control Applications, 1994.
[22] A. Raie, V. Rashtchi, Using a genetic algorithm for detection and magnitude determination of turn faults in an induction motor, Electrical Engineering 84 (5) (2002) 275–279.
[23] R. Isermann, Fault diagnosis of machines via parameter estimation and knowledge processing – tutorial paper, Automatica 29 (4) (1993) 815–835.
[24] R.H. Chen, J.L. Speyer, Generalized least-squares fault detection filter, International Journal of Adaptive Control and Signal Processing 14 (7) (2000) 747–757.
[25] S. Simani, C. Fantuzzi, Dynamic system identification and model-based fault diagnosis of an industrial gas turbine prototype, Mechatronics 16 (6) (2006) 341–363.
[26] E. Garcia Alcorta, P.M. Frank, Deterministic nonlinear observer-based approaches to fault diagnosis: a survey, Control Engineering Practice 5 (5) (1997) 663–670.
[27] O.A.Z. Sotomayor, D. Odloak, Observer-based fault diagnosis in chemical plants, Chemical Engineering Journal 112 (1–3) (2005) 93–108.
[28] A. Zolghadri, D. Henry, M. Monsion, Design of nonlinear observers for fault diagnosis: a case study, Control Engineering Practice 4 (11) (1996) 1535–1544.
[29] M. Zaheeruddin, N. Tudoroiu, Dual EKF estimator for fault detection and isolation in heating ventilation and air conditioning systems, in: IECON Proceedings (Industrial Electronics Conference), 2012, pp. 2257–2262.
[30] F.J. Uppal, R.J. Patton, Neuro-fuzzy uncertainty de-coupling: a multiple-model paradigm for fault detection and isolation, International Journal of Adaptive Control and Signal Processing 19 (2005) 281–304.
[31] V. Venkat, K. Chan, A neural network methodology for process fault diagnosis, AIChE Journal 35 (12) (1989) 1993–2002.
[32] J. Li, Y. Guo, J. Wall, S. West, Fault detection for HVAC systems, in: The 10th International Conference on Healthy Building, vol. 1, 2012, pp. 388–393.
[33] A. Akhenak, M. Chadli, et al., Fault Detection and Isolation using Sliding Mode Observer for Uncertain Takagi–Sugeno Fuzzy Model, Institute of Electrical and Electronics Engineers Computer Society, Ajaccio–Corsica, France, 2008.
[34] A. Hafaifa, F. Laaouad, et al., Fuzzy modelling and control for detection and isolation in industrial centrifugal compressors, Journal of Automatic Control 19 (2009) 19–26.
[35] B. Jiang, P. Shi, et al., Sliding mode observer-based fault estimation for nonlinear networked control systems, Circuits, Systems, and Signal Processing 30 (1) (2011) 1–16.
[36] I. Nagesh, C. Edwards, A Sliding Mode Observer Based FDI Scheme for a Nonlinear Satellite Systems, Institute of Electrical and Electronics Engineers Inc., Denver, CO, 2011.
[37] T. Takagi, M. Sugeno, Fuzzy identification of systems and its applications to modelling and control, IEEE Transactions on Systems, Man and Cybernetics – Part B: Cybernetics 15 (1) (1985) 116–132.
[38] D. Blake, M. Brown, Simultaneous, Multiplicative Actuator and Sensor Fault Estimation using Fuzzy Observers, Institute of Electrical and Electronics Engineers Inc., London, United kingdom, 2007.
[39] X. Yang, X. Jin, Z. Du, et al., Optimum operating performance based online fault-tolerant control strategy for sensor faults in air conditioning systems, Automation in Construction 37 (2014) 145–154.
[40] Y. Song, Y. Akashi, J. Yee, A development of easy-to-use tool for fault detection and diagnosis in building air-conditioning systems, Energy and Buildings 40 (2008) 71–82.
[41] D. Krokavec, A. Filasova, Estimation of Nonlinear System Parameter Faults via Sliding Mode Observer, IEEE Computer Society, Wuhan, China, 2011.
[42] I. Castillo, T.F. Edgar, B.R. Fernández, et al., Robust model-based fault detection and isolation for nonlinear processes using sliding modes, International Journal of Robust and Nonlinear Control 22 (1) (2012) 89–104.
[43] Q. Wu, M. Saif, A Neural-Fuzzy Sliding Mode Observer for Robust Fault Diagnosis, Institute of Electrical and Electronics Engineers Inc., St. Louis, MO, 2009.
[44] K.C. Veluvolu, Y.C. Soh, Fault reconstruction and state estimation with sliding mode observers for Lipschitz non-linear systems, IET Control Theory and Applications 5 (11) (2011) 1255–1263.
[45] X. Yang, X. Jin, Z. Du, et al., A hybrid model-based fault detection strategy for air handling unit sensors, Energy and Buildings 57 (2013) 132–143.
[46] D.P. Yuill, J.E. Braun, Evaluating the performance of fault detection and diagnostics protocols applied to air-cooled unitary air-conditioning equipment, HVAC and R Research 19 (7) (2013) 882–891.
[47] L. Wang, S. Greenberg, J. Fiegel, et al., Monitoring-based HVAC commissioning of an existing office building for energy efficiency, Applied Energy 102 (2013) 1382–1390.
[48] B.E. Postlethwaite, M. Brown, C.H. Sing, A new identification algorithm for fuzzy relational models and its application in model-based control, Transactions of the IChemE 75 (Part A) (1997) 453–458.
[49] J. Cheng, X. Yao, et al., Fuzzy sliding mode controller based on trending law for electric actuator, in: ISSCAA2010 – Third International Symposium on Systems and Control in Aeronautics and Astronautics, Harbin, China, IEEE Computer Society, 2010.
[50] D. Kukolj, E. Levi, Identification of complex systems based on neural and Takagi-Sugeno fuzzy model, IEEE Transactions on Systems, Man, and Cybernetics, Part B: Cybernetics 34 (1) (2004) 272–282.
[51] S. Rajaraman, J. Hahn, M.S. Mannan, A methodology for fault detection, isolation, and identification for nonlinear processes with parametric uncertainties, Industrial and Engineering Chemistry Research 43 (21) (2004) 6774–6786.
[52] A. Husaunndee, R. Lahrech, P. Riederer, H. Vaezi-nejad, SIMBAD Building and HVAC Toolbox, Version 3.0, Automation and Energy Management Group, CSTB, 2001.
[53] D. Ngo, A. Dexter, Fault diagnosis in air-conditioning systems with generic model of the HVAC plant, in: Proceedings of the 5th International Conference on System Simulation in Buildings, University of Liege, Liege, Belgium, 1998.
[54] Y. Zhou, A. Dexter, Estimating the size of incipient faults in HVAC equipment, HVAC and R Research 15 (1) (2009) 151–163.

[55] B. Kelkar, B. Postlethwaite, Enhancing the generality of fuzzy relational models for control, Fuzzy Sets Systems 100 (1998) 117–129.
[56] Y. Zhou, A. Dexter, Off-line identification of nonlinear, dynamic systems using a neuro-fuzzy modelling technique, Fuzzy Sets and Systems 225 (2013) 74–92.
[57] A. Dexter, J. Pakanen (Eds.), Demonstrating Automated Fault Detection and Diagnosis Methods in Real Buildings. VTT Building Technology, Espoo. VTT Symposium 217, 2001, 381 pp. + app. 13 pp.
[58] Y. Wu, A.L. Dexter, Modelling capabilities of fuzzy relational models, in: The IEEE International Conference on Fuzzy Systems, 2003.
[59] Y.-J. Huang, Y.-J. Wang, Steady-state analysis for a class of sliding mode controlled systems using describing function method, Nonlinear Dynamics 30 (3) (2002) 223–241.
[60] R. Thompson, A.L. Dexter, A fuzzy decision-making approach to temperature control in air-conditioning systems, Control Engineering Practice 13 (6) (2005) 689–698.